Chemical Reaction Effect in Mhd Slip Flow of Alumina Water Nanofluid Over a Flat Plate

Padam Singh[1] and Manoj Kumar[2]

[1]Department of Mathematics, Statistics and Computer Science,
[2]G.B. Pant University of Agriculture and Technology, Pantnagar, Uttarakhand, India

Email: tomar.padam@gmail.com, mnj_kumar2004@yahoo.com

Abstract: Present study deals with the investigation of chemical reaction effect in mass transfer of magnetohydrodynamic slip flow of laminar, electrically conducting, viscous, incompressible alumina water nanofluid over a flat plate. The governing equations are transformed into simultaneous ordinary differential equations by using appropriate similarity transformation. The set of equations thus obtained has been solved numerically by using Adaptive Runge-Kutta method and with shooting technique. The effects of chemical reaction rate and magnetic field on velocity, concentration, shear stress and concentration gradient have depicted graphically and analyzed. Significant changes were observed in the mass transfer rate with respect to these physical parameters.

Keywords: Magnetohydrodynamic, Nanofluid, Boundary Layer Slip, Volume Fraction, Concentration, Chemical reaction.

2010 Mathematics Subject Classification: 76V05, 76W05, 65L06, 76N20, 76D05

NOMENCLATURE

B	Magnetic field	γ	Velocity slip parameter
D_{nf}	Mass diffusivity	η	Non dimensional distance
G_c	Solutal Grashof number	ρ_f	Density of water
g	Gravitational acceleration	ρ_{nf}	Nanofluid density
k	Reaction rate	ρ_s	Density of alumina particles
L	Reference length	σ_{nf}	Electrical conductivity of nanofluid
M	Magnetic parameter	μ_{nf}	Dynamic viscosity of nanofluid
Sc	Schmidt Number	$\emptyset$	Volume fraction of nanoparticles
u_∞	Uniform free stream velocity	ψ	Stream function
u, v	Velocity components in x and y direction	χ	Non dimensional concentration
x, y	Coordinate axes	υ_{nf}	Kinematic viscosity of nanofluid
	Greek Symbol	ρ_f	Density of water

$(\beta_s)_{nf}$ Solutal expansion coefficient

1. INTRODUCTION

Anjali et. al. [2] gave an approximate solution for the steady laminar flow along a semi infinite horizontal plate in the presence of species concentration. The results were shown that the velocity and concentration increase with the decay of the Schmidt number, skin friction and rate of concentration decrease with the increase of chemical reaction parameter. Mamut [5] presented the results regarding characterization of nanofluid properties. The experimental results were compared with the theoretical simulation based on the assumptions regarding heat and mass transfer. Xuan [6] studied mass transfer in binary nanofluids and found that the nanoparticles improved the mass transfer inside binary nanofluids. Gorla and Chamkha [7] presented a boundary layer analysis for the natural convection past a horizontal plate in a porous medium saturated with a nano fluid. Numerical results for friction factor, surface heat transfer rate and mass transfer rate were presented. The dependency of the friction factor, surface heat transfer rate and mass transfer rate on these parameters were discussed. Bhattacharyya [8] was studied the boundary layer flow over a porous flat plate with diffusion of chemically reactive species undergoing first order reaction and subject to suction/injection. The study reveals that for the increase in suction at the plate, both velocity and concentration boundary layer thicknesses decrease and for increasing injection, both thicknesses increases. The rate of solute transfer from the plate increases with reaction rate parameter and power-law exponent. Aladag et. al. [9] presented experimental investigations of the viscosity of nanofluids at low temperatures. The experiments have also shown that CNT water based nanofluid behaves as Newtonian fluid at high shear rate whereas alumina water based nanofluid is non-Newtonian within the range of low temperatures investigated. Pang et. al. [10] studied the mass transfer enhancement by binary nanofluids for bubble absorption process. The results were shown that the mass transfer enhancement with coolant is more than compared to without coolant. Rout et. al. [11] investigated the influence of chemical reaction and the combined effects of internal heat generation and a convective boundary condition on the laminar boundary layer MHD heat and mass transfer flow over a moving vertical flat plate. The discussion was focused on the physical interpretation of the results as well as their comparison with previous studies which show good agreement as a special case of the problem.

The present investigation deals with study of chemical reaction effect in mass transfer of boundary layer slip flow of alumina-water nanofluid in the presence of magnetic field over a flat plate.

MATHEMATICAL FORMULATION

The physical model is given here along with flow configuration and coordinate system. The system deals with two dimensional boundary layer slip flow of water based nanofluid. A uniform magnetic field B is applied

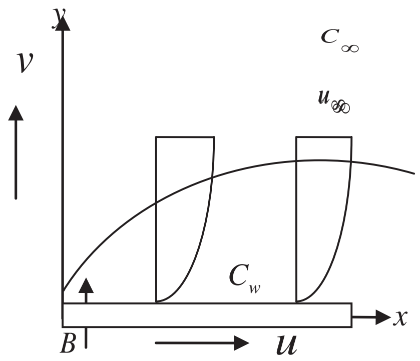

Figure 1: Physical model of the flow

in the transverse direction. The C_w and C_∞ denote the concentration at the surface and concentration at free stream respectively. The continuity, momentum and concentration equations representing flow are as following:

$$\frac{\partial u}{\partial x}+\frac{\partial v}{\partial y}=0 \quad (1)$$

$$u\frac{\partial u}{\partial x}+v\frac{\partial u}{\partial y}=\upsilon_{nf}\frac{\partial^2 u}{\partial y^2}+g(\beta_s)_{nf}(C-C_\infty)+\frac{\sigma_{nf}B}{\rho_{nf}}(u_\infty-u) \quad (2)$$

$$u\frac{\partial C}{\partial x}+v\frac{\partial C}{\partial y}=D_{nf}\frac{\partial^2 C}{\partial y^2}-k(C-C_\infty) \quad (3)$$

With the boundary conditions:

$$u=v_{sf}\frac{\partial u}{\partial y},\ v=0,\ C=C_W=C_\infty+C_0x^{\lambda}\ \text{ at } y=0 \text{ and}$$
$$u\to u_\infty,\ C\to C_\infty \quad \text{as } y\to\infty \quad (4)$$

Here $v_{sf}=v_0\sqrt{\frac{u_\infty x}{\upsilon_{nf}}}$ is velocity slip factor with initial value v_0 and λ is power index.

Table 1: Nanofluid properties:

Dynamic Viscosity [1]	$\mu_{nf}=\mu_f/(1-\emptyset)^{2.5}$
Density [3]	$\rho_{nf}=(1-\emptyset)\rho_f+\emptyset\rho_s$
Mass Diffusivity [4]	$D_{nf}=(1-\emptyset)D_f$
Kinematic Viscosity [5]	$\upsilon_{nf}=\mu_{nf}/\rho_{nf}$

Table 2: The physical properties of alumina and base fluid water at 20^{o}C:

	Density(Kg/m^3)	Mass Diffusivity (m^2/sec)	Dynamic Viscosity(Ns/m^2)
Water	1000.52	0.0000242	0.001002
Alumina	3970.0	-------------------	-----------------

2. METHOD FOR SOLUTION

To solve the governing equations (2) and (3) with the boundary conditions (4), following similarity transformation has been introduced:

$$\psi = \sqrt{u_\infty \upsilon_{nf} x}\ f(\eta),\ \eta = \frac{y}{x}\sqrt{\frac{x u_\infty}{\upsilon_{nf}}},\ \ \chi(\eta) = \frac{C - C_\infty}{C_w - C_\infty},\ \ M = \frac{\sigma x B^2}{u_\infty \rho_{nf}},\ \ R = \frac{L R_0}{U_\infty}\ \text{ and }\ G_c = \frac{g(\beta_s)_{nf}(C - C_\infty)x}{u_\infty^2}$$

where $B = \frac{B_0}{\sqrt{x}}$, $(\beta_s)_{nf} = \frac{\beta_0}{x}$, $Sc = \frac{\upsilon_{nf}}{D_{nf}}$ and $k = \frac{LR_0}{x}$ (5)

Here B_0, β_0 are constants and stream function ψ satisfies equation (1) with $u = \frac{\partial \psi}{\partial y}$ and $v = -\frac{\partial \psi}{\partial x}$

After using above transformation, the equations (2) and (3) reduced to the nonlinear differential equations as follows:

$$f'''(\eta) + \frac{1}{2} f(\eta) f''(\eta) + G_c\, \chi(\eta) - M\,(f'(\eta) - 1) = 0 \qquad (6)$$

$$\chi''(\eta) + \frac{1}{2} Sc\, f(\eta)\, \chi'(\eta) - Sc\, R\, \chi(\eta) = 0 \qquad (7)$$

and the boundary conditions (4) reduced as follows:

$$f(0) = 0\ ,\ f'(0) = \gamma f''(0),\ \ \chi(0) = 1 \text{ and } f'(\eta) \to 1,\ \chi(\eta) \to 0 \quad \text{when } \eta \to \infty \qquad (8)$$

Here $\gamma = \frac{V_0 u_\infty}{\upsilon_{nf}}$ is the velocity slip parameter.

Study of measure interest is to calculate shear stresses and Sherwood number (Sh) which are given as follows:

$$\tau = \left(\frac{\partial u}{\partial y}\right)_{y=0} \propto\ f''(0), \qquad Sh = -\left(\frac{\partial C}{\partial y}\right)_{y=0} \propto\ -\chi'(0)$$

To solve the non-linear differential equations (6) and (7) subject to the boundary conditions (8) adaptive Runge-Kutta method and with shooting technique has been applied. This method is based on the discretization of the problem domain and the calculation of unknown boundary conditions. The domain of the problem is discretized and the boundary conditions for $\eta = \infty$ are replaced by $f'(\eta_{max}) = 1$ and $\theta(\eta_{max}) = 0$ where η_{max} is sufficiently large value of η at which the boundary conditions (8) for $f(\eta)$ is satisfied. The nonlinear equations (6) and (7) first converted into five first order ordinary linear differential equations:

$$f'(\eta) = y(2); \quad f''(\eta) = y'(2) = y(3);$$

$$f'''(\eta) = y'(3) = \left[-\frac{1}{2}y(1)y(3) - M\{1 - y(2)\} - G_c\, y(4)\right]; \chi' = y(5);$$

$$\chi''(\eta) = y'(5) = \left[-\frac{1}{2}Sc\, y(1)y(5) + Sc\, R\, y(4)\right]$$

There are three conditions on the boundary $\eta = 0$ and two conditions at $\eta \to \infty$. To get the solution of the problem two more initial conditions have been found by shooting technique. The values of unknowns $f''(0)$ and $\chi'(0)$ at which solution agrees with the prescribed boundary conditions (8) has been tabulated in table 3.

Adaptive Runge-Kutta method estimates the truncation error at each integration step and automatically adjusts the step size to keep the error within prescribed limits. The formula used to measure the actual conservative error is defined by:

$$e(h) = \sqrt{\frac{1}{5}\sum_{i=1}^{5} E_i^2(h)}$$

Here $E_i(h)$ is the measure of error in the dependent variable y_i. Per-step error control is achieved by adjusting the increment h by $h_{i+1} = 0.9h_i(\varepsilon/e(h_i))^{1/5}$; $i = 1, 2, 3, 4, 5$ so that it is approximately equal to the prescribed tolerance $\varepsilon = 10^{-6}$. The assumed initial step size is $h = 0.01$.

Table 3: Values of $f''(0)$ and $-\chi'(0)$ obtained by shooting.

		Under boundary slip		No boundary slip	
Parameters		$f''(0)$	$-\chi'(0)$	$f''(0)$	$-\chi'(0)$
Reaction Rate parameter(R)	0.0	0.7771	0.2168	0.8118	0.2121
	0.1	0.7871	0.1785	0.8227	0.1733
	0.3	0.8138	0.0861	0.8517	0.0792
[$\gamma = 0.1$, $M = 0.2$, $G_c = 0.2$, $Sc = 0.2$]	0.5	0.8541	-0.0425	0.8951	-0.0512
Magnetic parameter(M)	0.0	0.7709	-0.0419	0.7935	-0.0509
	0.2	0.8539	-0.0419	0.8958	-0.0522
	0.5	0.9685	-0.0419	1.0358	-0.0499
	0.7	1.0378	-0.0419	1.1227	-0.0499
[$\gamma = 0.1$, $R = 0.5$, $Sc = 0.2$, $G_c = 0.2$]	1.0	1.13275	-0.0414	1.2439	-0.0499

3. RESULTS AND DISCUSSION

The computations have been made for velocity, shear stress, concentration and concentration gradient profiles and other parameters involved in the study. The results were depicted graphically and their physical explanations were also given corresponding to different values of reaction rate parameter and magnetic parameter.

Table 4: The values of physical parameters for Al_2O_3 water nanofluid at 20^0C corresponding to different volume fraction (ϕ):

Vol. Fr. ϕ	Density $[10^3 \rho_{nf}]$	Dynamic Viscosity μ_{nf}	Kinematic viscosity υ_{nf}	Mass Diffusivity $[10^{-4} D_{nf}]$	Schmidt Number $[10^4 Sc]$
0.00	1.0005200	0.001002000	1.001479230	0.2420000	4.138343928
0.01	1.0302148	0.001027495	0.997360009	0.2395800	4.162951870
0.02	1.0599096	0.001053907	0.994337243	0.2371600	4.192685291
0.03	1.0896044	0.001081280	0.992360656	0.2347400	4.227488523
0.04	1.1192992	0.001109659	0.991387515	0.2323200	4.267336069
0.05	1.1489940	0.001139091	0.991381813	0.2299000	4.312230591
0.06	1.1786888	0.001169628	0.992313570	0.2274800	4.362201382
0.07	1.2083836	0.001201324	0.994158265	0.2250600	4.417303233
0.08	1.2380784	0.001234235	0.996896351	0.2226400	4.477615662
0.09	1.2677732	0.001268423	1.000512857	0.2202200	4.543242471
0.10	1.2974680	0.001303951	1.004997062	0.2178000	4.614311582

Figures 2-5 exhibit the velocity, shear stress, concentration and concentration gradient profiles respectively, for various values of reaction rate parameter (i.e. R = 0, 0.1, 0.3, 0.5) in the presence and absence of boundary slip. It is noticed that in the figures 2 and 3, the velocity increases and the shear stress decreases with an increase in the reaction rate in both the cases. The concentration increases with an increase in the reaction rate in both the cases, concentration gradient increase upto $\eta = 2.6817$ in the presence of boundary slip and upto $\eta = 2.74$ in the absence of boundary slip and then decreases with an increment in the reaction rate as shown in figures 4 and 5. Figures 6-9 show the effect of magnetic parameter on velocity, shear stress, concentration and concentration gradient profiles respectively for magnetic parameter (M = 0, 0.2, 0.5, 0.7, 1) in both cases. It has been observed that the velocity increases with an increase in the magnetic parameter as shown in figure 6, and shear stress decreases with an increase in the magnetic parameter in both cases as shown in figure 7. The effect of magnetic parameter on concentration and concentration gradient also has been studied through figures 8 and 9. It is noticed that the concentration increases with an increase in the magnetic parameter in both cases. The concentration gradient increases up to $0 \leq \eta \leq 4.156$ in the presence of boundary slip and increases upto $0 \leq \eta \leq 4.213$ in the absence of boundary slip and then decreases as the value of magnetic parameter increases. Figures 10 -11 show the behavior of mass diffusivity, dynamic viscosity and Schmidt number, Kinematic viscosity corresponding to volume fraction.

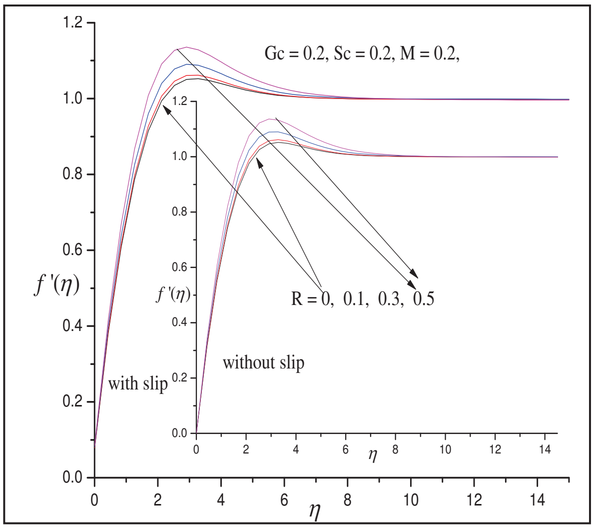

Fig.2: Effect of reaction rate parameter on velocity

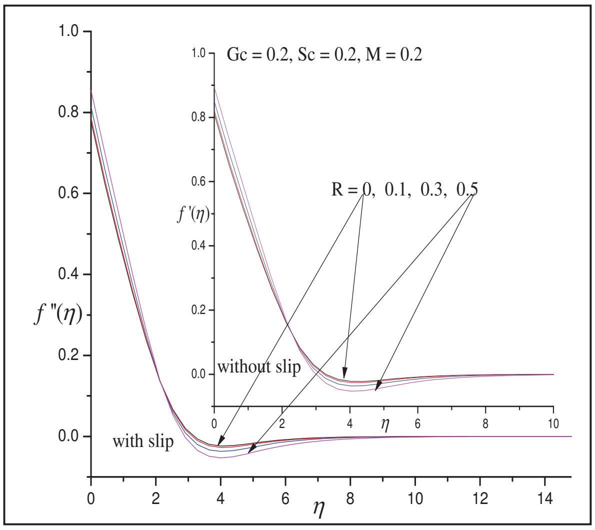

Fig.3: Effect of reaction rate parameter on shear stress

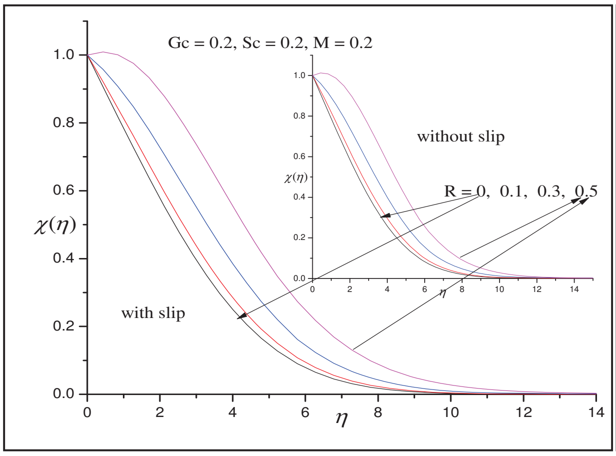

Fig.4: Effect of reaction rate parameter on concentration

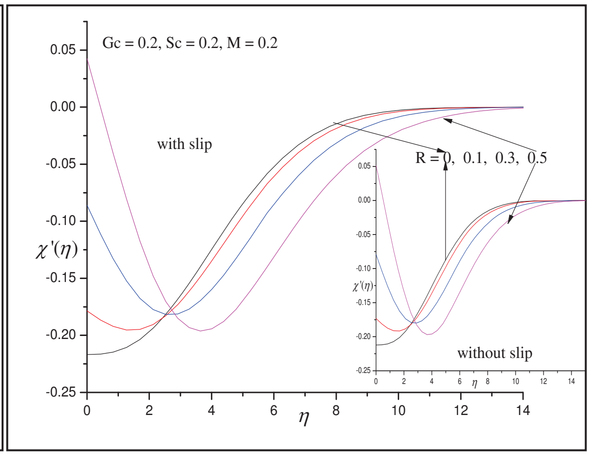

Fig.5: Effect of reaction rate parameter on concentration gradient

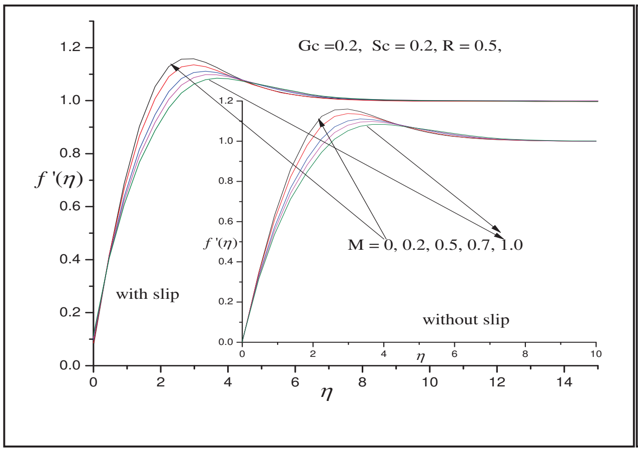

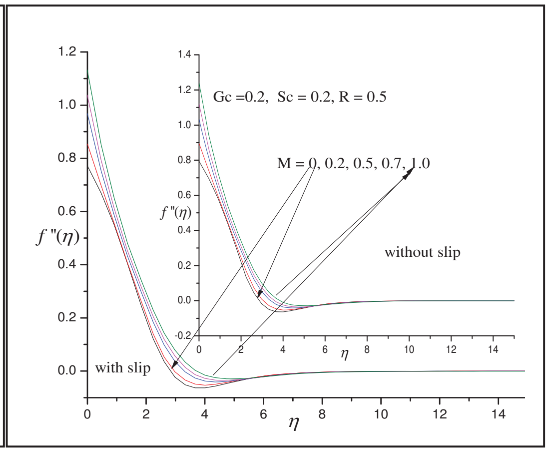

Fig.6: Effect of magnetic parameter on velocity profile

Fig.7: Effect of magnetic parameter on shear stress profile

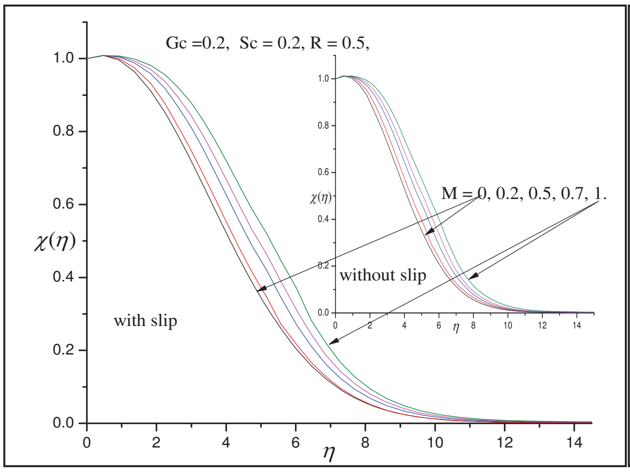

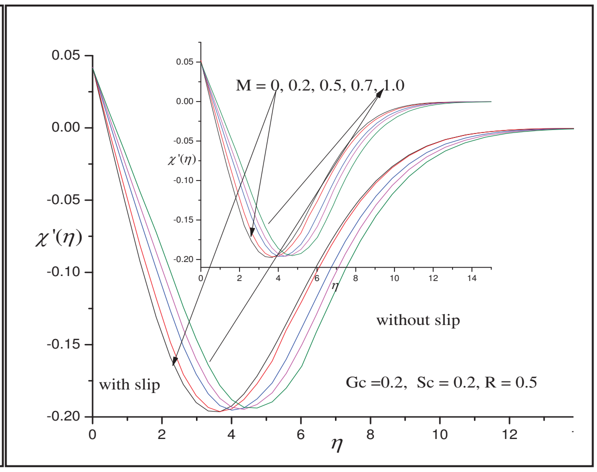

Fig.8: Effect of magnetic parameter on concentration

Fig.9: Effect of magnetic parameter on concentration gradient

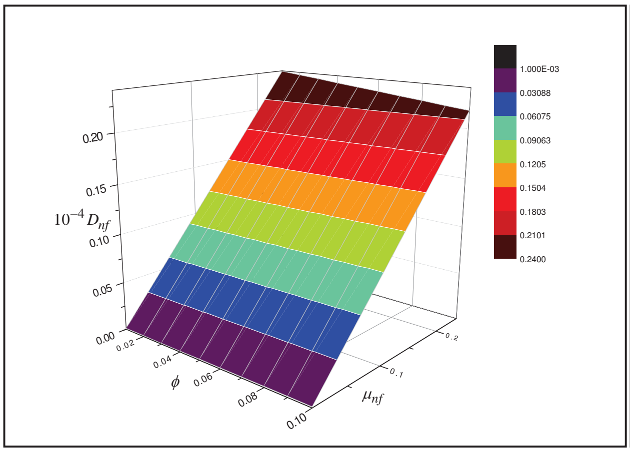

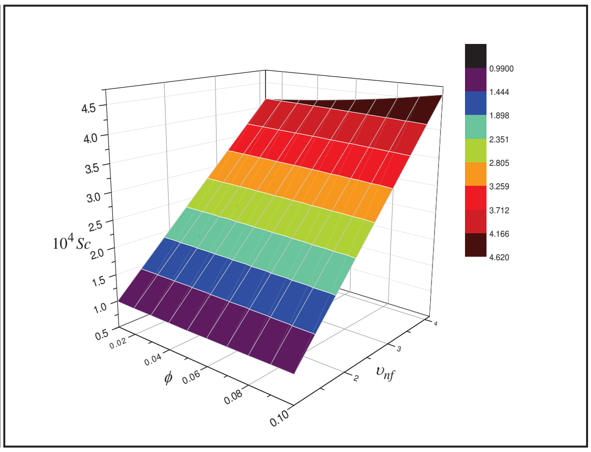

Fig.10: Vol. Fraction *vs* mass diffusivity and dynamic viscosity

Fig.11: Vol. Fraction *vs* Schmidt number and kinematic viscosity

References

[1] Einstein, A. Investigation on the Theory of the Brownian movement, *Dover, New York* (1956).

[2] Anjali devi, S.P. and Kandasamy, R. Effect of chemical reaction, heat and mass transfer on laminar flow along a semi infinite horizontal plate, *Heat and mass transfer*, 35(1999)

[3] Drew, D.A. and Passman, S.L. Theory of Multicomponent Fluids, *Springer* (1999), pp. 465-467.

[4] Kang, Y.T., King, J., Choi, C.K. Analysis of convective instabilities of binary nanofluids, *Int. refrigeration and air conditioning conference at Purdue,* July(2004), pp.12-15,

[5] Mamut, E. Characterization of heat and mass transfer properties of nanofluids, *Rom. J. Phys.,* (2006)51, pp.5-12.

[6] Xuan, Y. Conception for enhanced mass transport in binary nanofluids, *Heat mass transfer,* (2009) 46, pp.277-279.

[7] Gorla, R.S.R., Chamkha, A. Natural Convective Boundary Layer Flow over a Horizontal Plate Embedded in a Porous Medium Saturated with a Nanofluid, *Journal of Modern Physics,* 2(2011) pp. 62-71.

[8] Bhattacharyya, K . Boundary layer flow with diffusion and first order chemical reaction over a porous flat plate subject to suction/injection and with variable wall concentration, *Chemical engineering research bulletin*, 15(2011) pp. 6-11.

[9] Aladag, B., Halelfadl, S., Doner, N., Mare, T., Duret, S. and Estelle, P. Experimental investigations of the viscosity of nanofluids at low temperatures, *Applied Energy,* 97 (2012) pp. 876-880.

[10] Pang, C., Wu, W., Sheng, W., Zhang, H. and Kang, Y.T. Mass transfer enhancement by binary nanofluids for bubble absorption process, *Int. J.of Refrigeration*, (2012)35, pp.2240-2247.

[11] Rout, B.R., Parida, S.K. and S. Panda, S. MHD heat and mass transfer of chemical reaction fluid flow over a moving vertical plate in presence of heat source with convective surface boundary condition, *Hindawi publishing corporation international journal of chemical engineering*, (2013) Article ID 296834, pp. 1-11